Universiteit
Leiden
The Netherlands

Cholesterol metabolism in mouse models of atherosclerosis and adrenal steroidogenesis

Sluis, R.J. van der

Citation
Sluis, R. J. van der. (2020, November 19). *Cholesterol metabolism in mouse models of atherosclerosis and adrenal steroidogenesis*. Retrieved from https://hdl.handle.net/1887/138374

Version:	Publisher's Version
License:	Licence agreement concerning inclusion of doctoral thesis in the Institutional Repository of the University of Leiden
Downloaded from:	https://hdl.handle.net/1887/138374

Note: To cite this publication please use the final published version (if applicable).

Cover Page

Universiteit Leiden

The handle http://hdl.handle.net/1887/138374 holds various files of this Leiden University dissertation.

Author: Sluis, R.J. van der
Title: Cholesterol metabolism in mouse models of atherosclerosis and adrenal steroidogenesis
Issue date: 2020-11-19

2

DISRUPTION OF PLTP-MEDIATED HDL MATURATION REDUCES SR-BI DEFICIENCY-DRIVEN ATHEROSCLEROSIS SUSCEPTIBILITY DESPITE UNEXPECTED METABOLIC COMPLICATIONS

Ronald J. van der Sluis[1], Reeni B. Hildebrand[1], Bart Lammers[1], Sander Kooijman[2], Ying Zhao[1], Domenico Praticò[3], Matti Jauhiainen[4], Theo J.C. van Berkel[1], Patrick C.N. Rensen[2], Menno Hoekstra[1], Miranda van Eck[1]

ABSTRACT

BACKGROUND AND AIM: Functional loss of scavenger receptor class B, type I (SR-BI) in mice increases atherosclerosis susceptibility and stimulates accumulation of abnormally large HDL particles. A key modulator of HDL enlargement is phospholipid transfer protein (PLTP). In this study the importance of PLTP in SR-BI knockout (sKO) mice and the influence on the atherosclerosis susceptibility was investigated.

METHODS: Mice were fed a Western-type diet for 20 weeks to induce atherosclerosis.

RESULTS: In response to PLTP deficiency, a 1.7-fold ($P<0.001$) and 1.4-fold ($P<0.001$) decrease in serum cholesterol and phospholipid levels was found in sKO mice.
The lipoprotein distribution of cholesterol and phospholipids shifted from HDL to the VLDL/LDL fraction. Moreover, restoration of the HDL particle size was noted in the SR-BI/PLTP double KO (dKO) mice. Additional PLTP deficiency, however, did not normalize the impaired delivery of [^{3}H]cholesteryl esters from HDL to the liver. In line with the observed increase in VLDL levels, dKO mice also displayed a 2.2-fold ($P<0.001$) increase in serum triglycerides, which was accompanied by glucose intolerance and 1.4-fold increased body weight ($P<0.001$). Interestingly, despite the presence of a metabolic syndrome-like phenotype in dKO mice, atherosclerosis susceptibility was significantly lower as compared to sKO mice (dKO 63.0 ± 9.7*10^3 μm^2 vs sKO 117.2 ± 32.4*10^3 μm^2).

CONCLUSIONS: PLTP is essential for the accumulation of the abnormally large HDL particles in SR-BI KO mice. Importantly, deletion of PLTP does reduce the susceptibility to atherosclerosis in SR-BI KO mice despite the increase in levels of pro-atherogenic VLDL particles and the development of a metabolic syndrome-like phenotype.

INTRODUCTION

Low levels of high-density lipoprotein cholesterol (HDL-C) are associated with an increased risk for developing cardiovascular disease (CVD) and its underlying pathology, atherosclerosis [1-6]. Modulation of HDL-C in animal models, however, did not result in clear evidence that ApoA1/HDL raising strategies prevent atherosclerotic lesion development. Increasing the total amount of circulating HDL-C or ApoA1 (the main apolipoprotein on HDL) via, endothelial lipase inhibition [7,8] or by genetic modifications of genes involved in metabolism of HDL (lecithin cholesterol acyl transferase (LCAT)) overexpression [9] and scavenger receptor type B class 1 (SR-BI) deletion [10]) stimulated atherosclerotic lesion formation. In contrast, hepatic overexpression of human ApoA1 in mice and infusing the recombinant ApoA1milano phospholipid complex in cholesterol-fed rabbits did lower the risk for CVD [11-15]. Combined, these data indicate that interference early in the HDL metabolism lowers CVD risk, while increasing the circulating levels of HDL-C by blocking cholesteryl ester (CE) delivery to the liver (SR-BI KO) stimulates atherosclerotic lesion development. Clinical trials in humans using HDL-raising therapies did not give the desired reduction in the amount of cardiovascular events [16], including cholesteryl ester transfer protein (CETP) inhibition in the ILLUMINATE trail (Torcetrapib and Atorvastatin)[17], dal-OUTCOMES trail (Dalcetrapib)[18], AIM-HIGH trial (Niacin)[19] and the HPS2-THRIVE trail (Niacin+Laropiprant)[20]. In the DEFINE trail, the CETP inhibitor Anacetrapib did result in a minor reduction of the coronary lesion burden and a lower incidence of major coronary events [21]. Although Anacetrapib was effective in increasing HDL-cholesterol (+104 %) it cannot be excluded that the risk reduction was the consequence of an 18 % reduction in non-HDL-cholesterol.

The current hypothesis is that HDL's athero-protective properties are dependent on its functionality, not simply the amount of HDL-C in the circulation [21]. Although the knowledge on HDL metabolism and the link to atherosclerosis susceptibility has increased substantially in the past 2 decades, currently there are still large gaps in the general knowledge.

In human and rodent HDL metabolism, cell surface receptor SR-BI plays a predominant role. SR-BI is highly expressed in several cell types and tissues, like liver, macrophages [22] and steroidogenic tissues [23,24]. SR-BI facilitates the selective uptake of HDL-cholesteryl esters (HDL-CE) by hepatocytes [25] and mediates efflux of free cholesterol (FC) from peripheral tissues towards HDL [26] during the reverse cholesterol transport

(RCT) route. Screening of human subjects with elevated HDL-C levels revealed several mutations in the SR-BI gene. Vergeer et al. ([27] 2011) described a family with elevated HDL-C levels due to a missense mutation (P297S) in SR-BI. This mutation was associated with a reduction in cholesterol efflux from macrophages and decreased steroidogenesis. The number of carriers was, however, too low to demonstrate effects on cardiovascular events or carotid intima-media thickness. Various other identified mutations in the human SR-BI gene in subjects with elevated HDL-C levels further underline the role of SR-BI in human HDL metabolism (Zanoni et al. 2016 [28], Chadwick and Sahoo et al. 2012 [29], Brunham et al. 2011 [30], West et al. 2009 [31], Hsu et al. 2003 [32]).

To further understand the role of SR-BI in atherosclerotic lesion development and the RCT route, a total body knockout (KO) mouse was developed by the group of Monty Krieger [33]. They used a neo cassette mutagenesis strategy on the murine SCARB1 gene to generate knockout mice lacking functional SR-BI. SR-BI single knockout (sKO) mice display an impaired HDL-CE delivery to the liver and as a result increased HDL particle size and increased circulating HDL-C levels [33]. In line with these findings, studies using hepatic SR-BI overexpressing mice showed a reduction of HDL-C levels [34].
Despite the substantially increased HDL-C, SR-BI single knockout (sKO) mice are more susceptible to the formation of atherosclerotic lesions, indicating that its HDL is no longer athero-protective and displays most likely an altered functionality [35].

Currently, it is unknown if the increased susceptibility to atherosclerosis of SR-BI sKO mice is the consequence of the impairment of the last step of the RCT pathway and/or of the accumulation of the dysfunctional HDLs with an increased particle size. Therefore in this study, we aimed to block the remodelling of the HDL particles to specifically investigate the effects of the accumulation of the enlarged particles. A key modulator of HDL remodelling is phospholipid transfer protein (PLTP)[36-38]. PLTP belongs to a gene family of lipid transfer/lipopolysaccharide-binding proteins and facilitates the transfer of phospholipids, released during the lipolysis of triglyceride (TG)-rich particles, to pre-β-HDL particles. PLTP thereby enables the conversion of pre-β-HDL particles towards mature HDL particle subtypes [39,40].

We hypothesized that prevention of HDL particle enlargement in SR-BI sKO mice by deletion of PLTP function, will influence atherosclerosis susceptibility. By generation of SR-BI/PLTP double knockout (dKO) mice we show that PLTP is indeed essential for

the generation of the large CE-rich HDL particles in SR-BI sKO mice, but does not completely prevent atherosclerotic lesion development. Moreover, for the first time we provide proof that functional PLTP is essential for the lipolysis of TG-rich lipoproteins and that in absence of PLTP, VLDL triglycerides accumulate in the circulation of SR-BI sKO mice combined with the presence of a metabolic syndrome-like phenotype.

MATERIALS AND METHODS

ANIMALS

Heterozygous female SR-BI single knockout mice (SR-BI sKO, C57Bl/6 background) were kindly provided by M. Krieger. PLTP single KO mice (PLTP sKO, C57Bl/6 background) were kindly provided by M. Jauhiainen and crossbred to generate SR-BI/PLTP double KO (SR-BI/PLTP dKO) mice. Two independent animal experiments were performed: A) the lesion development study (wildtype (WT) n=5, SR-BI single knockout (sKO) n=5, SR-BI/PLTP dKO n=8) and B) the metabolic syndrome-like (MetS) phenotype study (WT n=8, SR-BI sKO n=5, PLTP sKO n=4, SR-BI/PLTP dKO n=7). Mice were given unlimited access to food and water and subjected to a 12 hour light/dark cycle. During the lesion development experiment (study A) mice were maintained on a regular chow diet (CHOW), containing 4.3 % (w/w) fat and no added cholesterol (RM3, Special Diet Services, Witham, UK) until the age of 14 weeks and subsequently challenged for a period of 20 weeks with semi-synthetic Western-type diet (WTD), containing 15 % (w/w) cacao butter, 1 % corn oil, 0.25 % (w/w) cholesterol, 20 % casein, 40.5 % sucrose, 5.95 % cellulose, 20 % corn-starch, 1 % choline chloride, vitamins and minerals (Diet W, Special Diet Services, Witham, UK) to induce atherosclerosis. During the MetS phenotype experiment (study B), all mice were on a regular CHOW diet up to the sacrifice at average 34 weeks of age. Animal experiments were performed at the Gorlaeus Laboratories of the Leiden Academic Centre for Drug Research. All animal work was approved by the Dutch Ethics Committee and regulatory authority at Leiden University and was carried out in compliance with Dutch government guidelines and the Directive 2010/63/EU of the European Parliament on the protection of animals used for scientific purposes.

HISTOLOGICAL ANALYSIS

To induce the development of atherosclerosis in the three valve area of the aortic root, WT, SR-BI sKO and SR-BI/PLTP dKO mice were fed WTD for 20 weeks. After sacrifice, the mice were perfused in situ with phosphate-buffered saline (100 mm Hg)

for 10 minutes via a cannula in the left ventricular apex. The heart plus aortic root were excised and stored in 3.7 % neutral-buffered formalin (Formal-fixx®, Shandon Scientific Ltd., UK) until further analysis. The mean atherosclerotic lesion area of each mouse was quantified from 10 oil red O-stained cryo-sections (10 µm), starting at the appearance of the tricuspid valves up to 300 µm of the ascending aorta using a Leica image analysis system, consisting of a Leica DMRE microscope coupled to a video camera and Leica Qwin Imaging software (Leica Ltd., Cambridge, UK).

After perfusion, a selection of organs (liver, spleen, adrenals, perigonadal white adipose tissue (pWAT), subcutaneous WAT (sWAT), interscapular brown adipose tissue (iBAT) were excised and weighed.

PLASMA LIPID ANALYSES

After a 4 hour fasting-period, approximately 100 µL blood was drawn from each individual mouse by tail bleeding and collected in ethylene diaminetetraacetic acid (EDTA)-coated tubes (Sarstedt, Numbrecht, Germany). Free cholesterol concentration in plasma was determined by an enzymatic colorimetric assay with 0.025 U/mL cholesterol oxidase (Sigma) and 0.065 U/mL peroxidase (Roche Diagnostics, Mannheim, Germany) in reaction buffer (1.0 KPi buffer, pH=7.7 containing 0.01 M phenol, 1 mM 4-amino-antipyrine, 1 % polyoxyethylene-9-laurylether, and 7.5 % methanol). Total cholesterol content was determined after addition of 0.003 U/mL cholesteryl esterase (Seikagaku Corporation, Japan), final absorbance was read at 490 nm. The distribution of cholesterol over the different lipoprotein particles in plasma was determined by fractionation of 30 µL plasma of each mouse using a Superose 6 column (3.2x300 mm, Smart-system, Pharmacia, Uppsala, Sweden). Total cholesterol content of the effluent was determined as above. VLDL-C, LDL-C, and HDL-C in plasma were calculated from the respective fractions (VLDL-C 2-6, LDL-C 7-11, and HDL-C 12-22). Percentual HDL and VLDL lipid composition was calculated after analysis of the free cholesterol, cholesteryl ester, phospholipids, and triglyceride content of pooled FPLC fractions corresponding to the HDL or VLDL peak. Phospholipids (Instruchemie, Delfzijl, The Netherlands) and triglycerides (Roche Diagnostics, Mannheim, Germany) were determined by enzymatic colorimetric assays according to manufacturer's instructions.

BLOOD CELL ANALYSIS

Blood was collected in ethylene diaminetetraacetic acid (EDTA)-coated tubes (Sarstedt, Numbrecht, Germany) by tail bleeding of mice after a 4 hour fasting-period. Whole blood samples (85 µL) were measured from mice on CHOW diet and on WTD,

using an automated veterinary hematology analyzer, Sysmex XT-2000iV (Goffin Meyvis, Etten-Leur, the Netherlands) to investigate blood cell counts.

ANALYSIS OF GENE EXPRESSION BY REAL-TIME QUANTITATIVE PCR

Quantitative gene expression was performed as previously described by Hoekstra et al. [41]. In summary, total RNA was isolated using a standard phenol/chloroform extraction method and reversely transcribed using RevertAid Reverse Transcriptase. Gene expression of analysis was performed by using SYBR-Green technology (Eurogentec). Primers were validated for an equal efficiency. Ratios of the target gene expression were determined by subtracting the Ct of the target gene from the Ct of the housekeeping gene and raised by 2 to the power of this difference. The target gene expression is thus relative to the housekeeping gene expression. Glyceraldehyde 3-phosphate dehydrogenase (GAPDH), ribosomal protein lateral stalk subunit P0 (36b4) were used as the housekeeping genes.

GLUCOSE TOLERANCE TEST

Mice were weighed and fasted 4 hours prior to administration of the glucose bolus of 2 g/kg per orally. Blood glucose was measured in time at 15, 30, 60, 120, 180, and 360 minutes after administration with a Roche accu-check mobile system.

ISOLATION OF PERITONEAL CELLS AND CHOLESTEROL EFFLUX

A cohort of chow-fed 12-week old female C57Bl6 mice were intra-peritoneally injected with 3 % Brewer's thioglycollate medium to induce the infiltration of macrophages into the peritoneal cavity. At 5 days after injection, the peritoneal cavity of the mice was lavaged with 10 mL cold PBS to collect thioglycollate-elicited peritoneal leukocytes [42].

To measure the cholesterol efflux capacity of the cells, thioglycollate-elicited peritoneal macrophages were incubated with 0.5 μCi·mL−1 [^{3}H]-cholesterol in DMEM/0.2 % BSA (fatty acid free) for 24 hours at 37 °C. Cholesterol efflux was studied by incubation of the cells with DMEM/0.2 % BSA or with 2.5 % serum of either WT, SR-BI sKO of SR-BI/PLTP dKO as lipid acceptors. Radioactivity in the medium and the cells was determined by scintillation counting after 24 hours of incubation. Cholesterol efflux was calculated as the amount of radioactivity in the medium compared with the total amount of radioactivity measured in medium plus cells.

MEASUREMENT OF ISOPROSTANES AND CARBONYLS

Serum, hepatic, splenic, and aortic arch isoprostane 8,12-iso-iPF2α-VI levels were measured by gas chromatography-mass spectrometry as described previously [43]. Blood samples were drawn, centrifuged at 7.000 rpm for 10 min, and serum was separated and stored at -80 °C until analysis. Samples were spiked with a known amount of internal standard, extracted and purified by thin-layer chromatography, and analysed by negative ion chemical ionization gas chromatography-mass spectrometry. The aortic arch, liver, and spleen from each individual mouse was obtained, weighed, minced, and homogenized in PBS containing EDTA (2 mM) and butylated hydroxytoluene (2 mM), pH 7.4, and total lipid was extracted using Folch solution (chloroform-methanol, 2:1, v/v). Next, base hydrolysis was performed using 15 % KOH at 45 °C for 1 hour, and the total levels of 8,12-iso-iPF2α-VI were processed before analysis as described above. Total protein carbonyls were determined by using the Zenith test kit according to the manufacturer's instructions (Zenith Technology, Dunedin, New Zealand) [44].

ISOLATION AND [^{3}H]CET-LABELING OF HDL

HDL needed for the [^{3}H]CEt -HDL clearance was isolated from healthy subjects and isolated via differential ultracentrifugation as described by Redgrave, Roberts and West [45]. Hereto the blood was dialyzed against PBS with 1 mM EDTA and the HDL fraction ($1.063<d<1.21$) was labeled with [^{3}H]CEt via exchange from donor particles. Donor particles were formed by sonication of egg yolk phosphatidylcholine supplemented with 50 µCi [^{3}H]CEt. Sonication was carried out with a Soniprep 150 (MSE Scientific instruments UK) for 40 min at 52 °C under a constant stream of argon in a 0.1 M KCl, 10 mM Tris, 1 mM EDTA, 0.025 % NaN_3 buffer (pH 8.0). Donor particles with a density of 1.03 g/ml were isolated by density gradient centrifugation in a Beckman SW 40Ti rotor. HDL was labeled by incubating HDL with donor particles (mass ratio of HDL protein/particle phospholipid 8:1) in the presence of human lipoprotein-deficient serum as the CE transfer protein source (1:1, v/v) for 8 h at 37 °C in a shaking-water bath under argon. Ethylmercurithiosalicylate (thimerosal; 20 mM) was added to stimulate CE transfer and to inhibit phospholipid transfer and lecithin:cholesterol acyltransferase activity. Radiolabeled HDL was then isolated by density gradient ultracentrifugation. The specific activity varied between 5 and 8 dpm/ng protein.

IN VIVO CLEARANCE AND LIVER UPTAKE OF [^{3}H]CET LABELED HDL

To study the clearance of the [^{3}H]CEt labeled HDL, a dose of 215 µg apolipoprotein (± $1.2x10^6$ dpm) of [^{3}H]CEt-HDL (total volume of 200 µL) was injected into the tail vein of WT, SR-BI sKO, and SR-BI/PLTP dKO mice. At 5 min after injection, a blood sample

was drawn to verify the injected dose. At 1, 2, 4, 6, 8 and 24 hours after injection blood samples were drawn to measure serum decay. Lipoprotein distribution of [^{3}H]CEt-HDL was determined at 8 hours after injection by fractionation of 110 µL serum of a pool of three mice using a Superose 6 column (3.2x300 mm, Smart-system, Pharmacia, Uppsala, Sweden). For analysis of liver association, the liver was excised at 24 h after tracer injection and overnight dissolved at 55 °C in Solvable (PerkinElmer), and [^{3}H] activity was quantified. Uptake of [^{3}H]CEt-HDL derived radioactivity by the liver was expressed per gram wet tissue weight and a correction was made for the radioactivity in the blood present in the liver at the time of sampling as determined by injection of screened [^{3}H]BSA (84.7 µL/g wet weight).

PREPARATION OF RADIOLABELED TRIGLYCERIDE-RICH LIPOPROTEINS (TRL)-MIMICKING EMULSION PARTICLES

Radiolabeled TRL-mimicking emulsion particles were prepared from 100 mg of total lipid including triolein (70 mg), egg yolk phosphatidylcholine (22.7 mg), lysophosphatidylcholine (2.3 mg), cholesteryl oleate (CO, 3.0 mg), and cholesterol (2.0 mg), with addition of [^{3}H]triolein (TO) (100 µCi) and [^{14}C]CO (10 µCi). Sonification was performed using a Soniprep 150 (MSE Scientific Instruments, UK) that is equipped with a water bath for temperature (54 °C) maintenance, at 10 µm output [46]. The emulsion was fractionated by consecutive density gradient ultracentrifugation steps in a Beckman SW 40 Ti rotor. After centrifugation for 27 min at 20,000 rpm at 20 °C, an emulsion fraction containing chylomicron-like particles (average size 150 nm) was removed from the top of the tube by aspiration and replaced by NaCl buffer (1.006 g/ml). After a subsequent centrifugation step for 27 min at 40,000 rpm, large VLDL-like particles (average size 80 nm) were obtained in a similar manner. Emulsions were stored at 4 °C under argon and used for in vivo kinetic experiments within 5 days following preparation.

IN VIVO CLEARANCE AND ORGAN UPTAKE OF RADIOLABELED TRL-MIMICKING EMULSION PARTICLES

To study the in vivo clearance of radio-labeled TRL-mimicking emulsion particles, mice were fasted for 4 hours and injected intravenously with 200 µl of emulsion particles with an average size of 80 nm (0.2 mg triglyceride (TG) per mouse). Blood samples were taken from the tail vein at 2, 5, 10, and 15 min after injection to determine the plasma decay of either [^{3}H]TO and [^{14}C]CO [47]. After taking the last blood sample, mice were euthanized by cervical dislocation and perfused with ice-cold PBS containing via the left ventricle of the heart to remove blood and non-internalized TRL-mimicking

particles from the organs. Subsequently, the liver, heart, spleen, hind limb muscle, gonadal WAT, subcutaneous WAT, interscapular BAT, adrenals and thymus were collected. Organs were dissolved overnight at 55 °C in Solvable (PerkinElmer), and [^{3}H] and [^{14}C] activity were quantified. Uptake of [^{3}H]TO- and [^{14}C]CO-derived radioactivity by the organs was expressed per gram wet tissue weight.

STATISTICAL ANALYSES

Statistical analyses were performed utilising the unpaired Student's t-test and one-way analysis of variance (ANOVA) after confirmation of Gaussian distribution using the test of Kolmogorov and Smirnov (Instat GraphPad software, San Diego, USA). A Grubbs outlier test was performed via Graphpad Quickcalcs online software. A Bonferroni post comparison test was executed after the ANOVA. The probability level for statistical significance (P) was set at 0.05 and the results are expressed as an average of standard error of the mean (SEM).

RESULTS

HDL particle size reduction and increased plasma triglycerides in CHOW-fed SR-BI/PLTP dKO mice.

In accordance with previously described studies [48,49] CHOW-fed SR-BI sKO mice displayed increased serum total cholesterol levels (TC 2.5-fold; P<0.005 vs WT), free cholesterol (FC 5.4-fold, P<0.005 vs WT), phospholipids (PL 1.3-fold; P<0.001 vs WT), triglycerides (TG 1.3-fold; P<0.05 vs WT) and free cholesterol/cholesteryl ester ratio (FC/CE ratio 4.5-fold; P<0.001 vs WT) (**Table 1**). Furthermore, lipoprotein fractionation (by FPLC) confirmed an increased HDL-C amount (area under the curve (AUC) SR-BI sKO 138 ± 4.2 vs WT 50 ± 1.7; P<0.001) alongside a left-shifted HDL peak, indicative for enlarged HDL particles (**Figure 1A CHOW**). These specific SR-BI sKO phenotypes were partly normalized in the SR-BI/PLTP dKO group. Compared to SR-BI sKO mice, serum TC and FC levels were significantly lower in the SR-BI/PLTP dKO group (TC 0.7-fold; P<0.01; FC 0.7-fold; P<0.01 vs SR-BI sKO). However, the FC/CE ratio in the SR-BI/PLTP dKO mice was not reduced (FC/CE ratio 4.0-fold vs WT; P<0.001). Circulating TG (TG 0.8-fold; P<0.05 vs SR-BI sKO) as well as the serum phospholipids (PL 0.75-fold; P<0.005 vs SR-BI sKO) were also decreased in the SR-BI/PLTP dKO mice versus the SR-BI sKO mice (**Table 1**). Furthermore, FPLC analysis showed a lower HDL-C peak with a right shift towards smaller sized particles and a decreased AUC in SR-BI/PLTP dKO

mice as compared to SR-BI sKO animals (AUC SR-BI/PLTP dKO 69 ± 2.2 vs 138 ± 4.2 SR-BI sKO; P<0.0001) (**Figure 1A CHOW**).

In mice, PLTP regulates the transfer of phospholipids needed for HDL particle maturation during the lipolysis of triglycerides in ApoB containing lipoproteins, like VLDL [50]. In line with this, a concomitant 3.5-fold increase in the AUC of the non-HDL fraction was observed in the SR-BI/PLTP dKO mice (AUC: SR-BI/PLTP dKO 19.0 ± 1.6; SR-BI sKO 5.5 ± 0.6; P<0.05) (data not shown).

HDL particles play a distinct role in the reverse cholesterol transport route from non-hepatic peripheral tissues towards the liver. The cholesterol efflux capacity of macrophages on the one hand and hepatic cholesterol uptake capacity on the other hand are important determinants of the effectivity of the reverse cholesterol transport route. Normalization of the cholesterol levels and reduction of the HDL particle size upon deletion of PLTP in SR-BI sKO mice did affect the capacity of serum to stimulate efflux of cholesterol from lipid-loaded wildtype macrophages in vitro (**Figure 2A**). In line with previous data [51], plasma from SR-BI sKO showed a decreased efflux capacity versus plasma from WT mice. Cholesterol efflux towards SR-BI/PLTP dKO plasma was improved, although not fully restored to WT level (WT 42.5 %, SR-BI sKO 30.3 %, SR-BI/PLTP dKO 35.9 %, all data sets are pooled plasma) (**Figure 2A**).

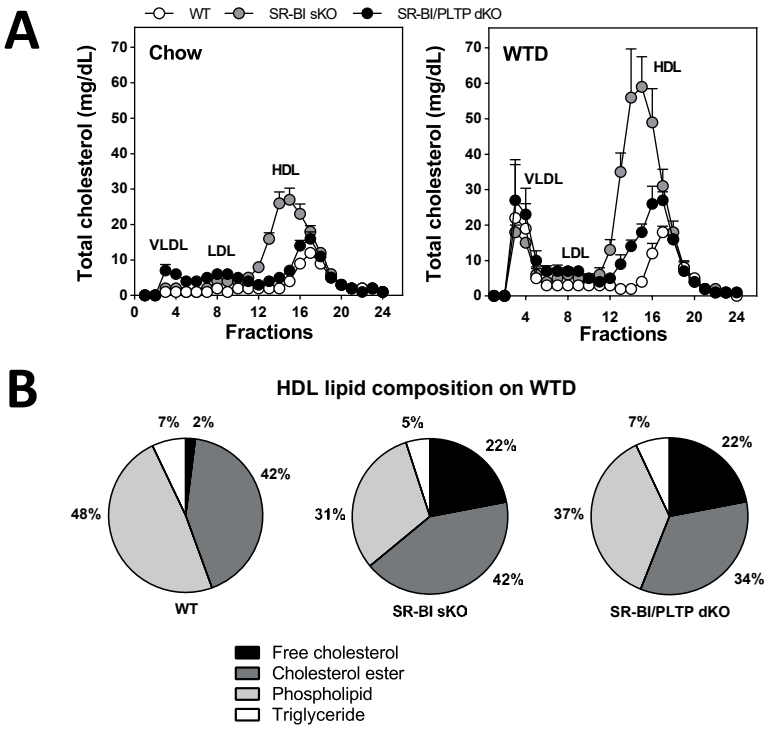

Figure 1: Plasma cholesterol lipid distribution of wild type (open circle), SR-BI sKO (grey circle),SR-BI/PLTP dKO (black circle) on either CHOW (WT n=4, sKO n=5, dKO n=8) or 20 weeks on Western type diet (WTD; amount of animals in all groups was 4), data represents mean+SEM (A). HDL composition (fractions 12-22) upon WTD challenge in % (B).

In vivo, labeled [^{3}H]-cholesteryl ether ([^{3}H]CEt) HDL injections showed that the disturbed serum clearance and hepatic uptake as a result of hepatic SR-BI deficiency was not restored by deletion of PLTP (% injected dose (ID) [^{3}H]CEt in the circulation at 24 hours after injection: SR-BI sKO 19.1 ± 1 %; SR-BI/PLTP dKO 17.4 ± 2 %; WT 3.6 ± 2 %; SR-BI sKO and SR-BI/PLTP dKO P<0.005 vs WT) (**Figure 2B**) (Hepatic uptake as % ID [^{3}H]CEt; SR-BI sKO 9 ± 0.4 %; SR-BI/PLTP dKO 9 ± 1 % vs WT 46 ± 2 %; P<0.0001) (**Figure 2C**).

In conclusion, under CHOW-fed conditions, deletion of PLTP in SR-BI KO mice limits the supply of phospholipids for the formation of the enlarged HDL particles caused by the absence of SR-BI on the liver. Moreover, HDL-C normalization in SR-BI KO mice by deletion of PLTP resulted in a slight improvement of plasma efflux capacity in vitro but did not restore the [^{3}H]CEt hepatic uptake in vivo.

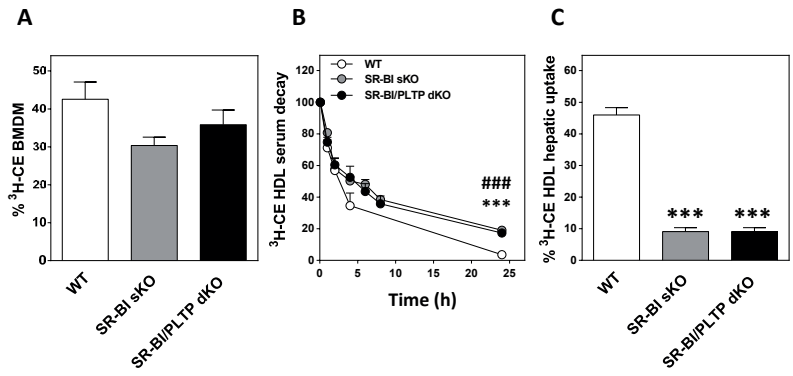

Figure 2: In vitro efflux from cholesterol loaded C57Bl6 bone marrow derived cells (BMDM) towards serum of either WT, SR-BI sKO or SR-BI/PLTP dKO mice on CHOW diet (A). Serum decay of [^{3}H]CE labeled HDL post IV injection of wild type (WT; open circles, n=3), SR-BI sKO (SR-BI sKO; gray circles, n=3) and SR-BI/PLTP dKO (SR-BI/PLTP dKO; black circles, n=3) data represents mean+SEM. Significant difference at the 24 hr time point; ***P<0.005 vs wild type; ###P<0.005 vs SR-BI sKO (B). Liver uptake of [3H]CE labeled HDL, data represents mean+SEM (WT n=5, SR-BI sKO n=5, SR-BI/PLTP dKO n=8, ***P<0.005 SR-BI vs WT, ***P<0.005 SR-BI vs WT) (C). Data represents mean+SEM.

HDL particle size reduction in SR-BI sKO mice did not recover SR-BI sKO blood phenotype on WTD.

To induce atherosclerotic lesion formation, mice were subsequently challenged with a Western-type diet (WTD) for a period of 20 weeks. Over time the serum TC levels increased in the SR-BI sKO group by 2.4-fold (P<0.001) (**Table 1 WTD**) and WTD feeding aggravated the SR-BI sKO HDL-C phenotype (AUC SR-BI sKO 269.5 ± 14.6; WT 71.0 ± 3.2 P<0.001) (**Figure 1 WTD**). The additional PLTP deletion resulted in significantly lower TC (1.7-fold; P<0.005), FC (1.7-fold; P<0.005), and PL (1.4-fold; P<0.005) levels versus SR-BI sKO WTD-fed mice (**Table 1 WTD**). Notably, deletion of PLTP also did not normalize the augmented plasma FC/CE ratio during the WTD challenge (4.0-fold; P<0.001 versus WT). On WTD, however, the clear reduction in HDL-C particle size and amount remained evident (AUC SR-BI/PLTP dKO 126.0 ± 5.0 vs SR-BI sKO 269 ± 14.6; P<0.001). The HDL particle lipid composition analysis showed an 11-fold increase in FC content in HDL of SR-BI/PLTP dKO mice versus WT mice, a phenotype similar to SR-BI sKO animals (**Figure 1B**).

Meurs et al. previously showed that the augmented FC levels in SR-BI sKO mice result in FC-enriched erythrocytes that have an augmented turnover and consequently

leading to an increased spleen size and higher reticulocyte counts in the sKO animals [49]. Another SR-BI sKO-specific blood phenotype are decreased platelet counts due to the increased FC content [52]. Here we confirmed these SR-BI sKO phenotypes, including higher reticulocyte count (SR-BI sKO 21.39 ± 2.4 $*10^{12}$/L vs 3.68 ± 1.0 $*10^{12}$/L in WT; P<0.0001), an enlarged spleen size (SR-BI sKO 301 ± 81 mg vs WT 185 ± 34 mg; P<0.05), and reduced platelet counts (SR-BI sKO 358.3 ± 30 $*10^{9}$/L vs WT 551.8 ± 83 $*10^{9}$/L; P<0.05). These phenotypes were not improved upon additional deletion of PLTP (reticulocyte count SR-BI/PLTP dKO 18.0 ± 1.0 $*10^{12}$/L; spleen SR-BI/PLTP dKO 255 ± 19 mg; platelet count SR-BI/PLTP dKO 317.9 ± 26 $*10^{9}$/L) (**Figure 3A, B, C**). Strikingly, upon WTD challenge, deletion of PLTP in the SR-BI sKO mice resulted in an increased WBC count, driven by a 1.4-fold increase in lymphocytes compared to SR-BI sKO (SR-BI/PLTP dKO 12.3 ± 1.1 $*10^{9}$/L vs SR-BI sKO 8.8 ± 0.9 $*10^{9}$/L and WT 6.7 ± 0.7 $*10^{9}$/L; P<0.01). Besides the increased lymphocyte count, deletion of PLTP in SR-BI KO mice resulted in a 2.2-fold increase in neutrophils (SR-BI/PLTP dKO 2.80 ± 0.24 $*10^{9}$/L; SR-BI sKO 1.50 ± 0.21 $*10^{9}$/L; WT 1.31 ± 0.16 $*10^{9}$/L; WT vs SR-BI sKO P=0.05; WT vs SR-BI/PLTP dKO P<0.005; SR-BI sKO vs SR-BI/PLTP dKO P<0.01) (**Figure 3D, E, F**). Combined these effects on blood cell counts suggest an increased inflammatory status in the SR-BI/PLTP dKO mice.

HDL particle size reduction by PLTP deletion in SR-BI KO mice lowers WTD-induced atherosclerosis susceptibility.

Next, the effect on atherosclerotic lesion development was investigated. In line with our previous study [35], WTD feeding for a period of 20 weeks induced the development of atherosclerotic lesions in the aortic root of SR-BI sKO mice, but not in WT controls (SR-BI sKO: 117 ± 32 $*10^{3}$ μm2; WT 1 ± 0.1 $*10^{3}$ μm^2; P<0.01). Normalization of the HDL-C levels, HDL particle size and the partly recovered efflux capacity in the SR-BI/PLTP dKO mice, was associated with 46 % smaller aortic root lesions in SR-BI/PLTP dKO mice versus SR-BI sKO mice (SR-BI/PLTP dKO 63 ± 7 $*10^{3}$ μm^2; t-test P<0.05 vs sKO, ANOVA P=NS) (**Figure 4A, C**), despite the increased inflammatory status. The lesion composition analysis revealed that the decreased lesion size in dKO group was paralleled by a diminished collagen content (SR-BI/PLTP dKO 16 ± 6 $*10^{3}$ μm^2; SR-BI sKO 44 ± 15 $*10^{3}$ μm^2; WT 1 ± 0.4 $*10^{3}$ μm^2, P=0.45 dKO vs sKO, P=0.98 dKO vs WT, P=0.13 WT vs dKO) (**Figure 4B, D**).

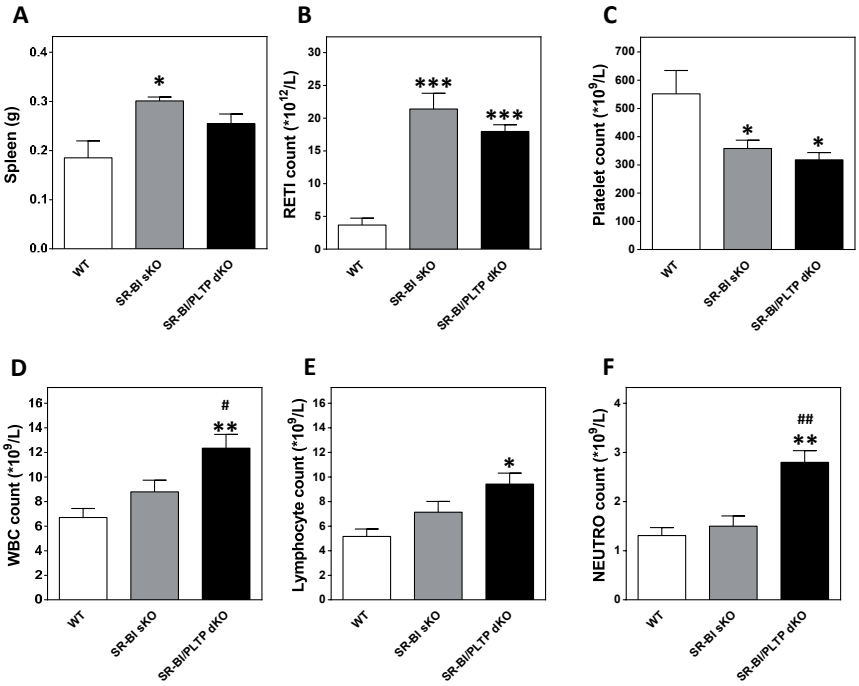

Figure 3: The effect of total body depletion of SR-BI sKO and additional PLTP depletion (SR-BI/PLTP dKO) post overnight fasted conditions on spleen weight (A), reticulocyte counts (RETI) (B),platelet counts (C), white blood cell count (WBC)(D), lymphocyte counts (E), neutrophil counts (NEUTRO)(F). All data represents mean+SEM, *P<0.05, **P<0.01 ***P<0.005 vs Wild type (WT) plasma, #P<0.05, ##P<0.01 vs SR-BI sKO.

In SR-BI sKO mice, the increased susceptibility for atherosclerosis is not only attributed to the impairment of the reverse cholesterol transport process, but also to increased oxidative stress as a result of the dysfunctional anti-oxidant activity of its abnormal HDL particles [53]. To investigate if reduction of HDL-C size by deletion of PLTP in SR-BI KO mice also restored in vivo oxidative stress levels as a measure of increased HDL functionality, we measured F2-isoprostane and carbonyl levels as markers of lipid and protein oxidation, respectively [54]. As previously described [53], SR-BI sKO animals showed increased plasma F2-isoprostanes (SR-BI sKO 415 ± 64 pg/mL compared to 153 ± 7 pg/mL in WT; P<0.01). The additional PLTP deletion in the SR-BI KO mice did not normalize the plasma F2-isoprostane levels (SR-BI/PLTP 338 ± 12 pg/mL, P<0.01 vs WT). Interestingly, local oxidative stress levels in the aortic arterial wall were normalized

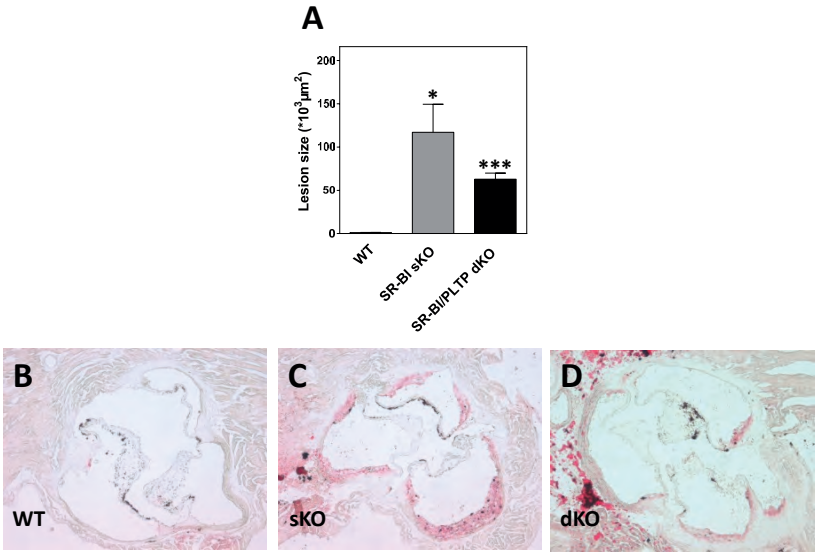

Figure 4: The effect on atherosclerosis lesion development in 20 weeks on Western type diet and overnight fasted conditions (A). Representative ORO positive lesions in the tree valve area per group at a 5x magnification (B). Massons trichrome positive collagen content in the lesion (C). Representative MT positive lesions in the tree valve area per group at a 5x magnification (D). WT (white bar n=5), SR-BI sKO (grey bar n=5) and SR-BI/PLTP dKO (black bar n=8). Statistically significant difference is at *P<0.05 **P<0.01 vs WT; #P<0.05 vs SR-BI sKO).

in the SR-BI/PLTP dKO group. Aorta F2-isoprostane levels were lowered 3.4-fold from 41 ± 3 pg/mg tissue in SR-BI sKO to 12 ± 2 pg/mg tissue (P<0.001) in the SR-BI/PLTP dKO mice as compared to 14 ± 3 pg/mg tissue in WT animals. An identical fold change was seen for carbonyls in aortic tissue, where SR-BI sKO mice had increased carbonyls (SR-BI sKO 0.48 ± 0.08 nmol/mg tissue; P<0.05) as compared to WT (WT 0.22 ± 0.04 nmol/mg tissue). PLTP deficiency normalized the carbonyl level to 0.2 ± 0.04 nmol/mg tissue (P<0.01 compared to SR-BI sKO group) in SR-BI/PLTP dKO mice (**Figure 5A, B, C**).

PLTP deletion in SR-BI sKO mice resulted in a metabolic syndrome-like phenotype driven by a misbalance in TG metabolism.

A prominent finding was that the SR-BI/PLTP dKO mice became severely obese over the period of 20 weeks WTD challenge (**Figure 6B**). At the end of the diet feeding period the body weight (BW) of the SR-BI/PLTP dKO mice as compared to both WT

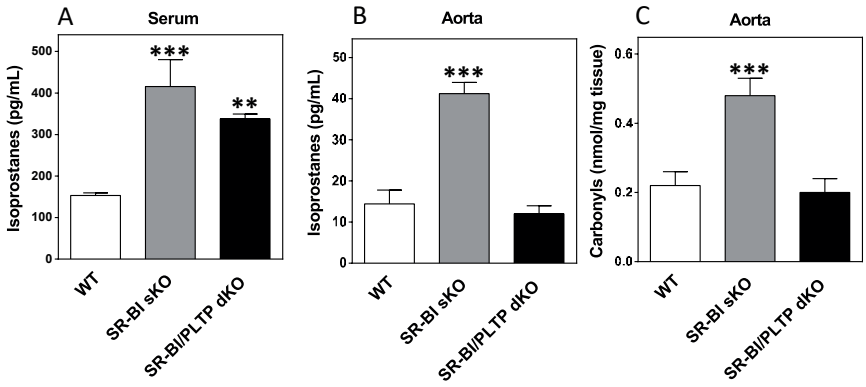

Figure 5: The effect of total body depletion of SR-BI (SR-BI sKO) and additional PLTP depletion (SR-BI/PLTP dKO) on (A) oxidative stress levels measured in 20 weeks on Western type diet female mice in serum and (B&C) aorta tissue. Data represents mean+SEM (WTD n=5, SR-BI sKO n=5 and SR-BI/PLTP dKO n=8). Statistical difference of **P<0.01, ***P<0.01 vs WT.

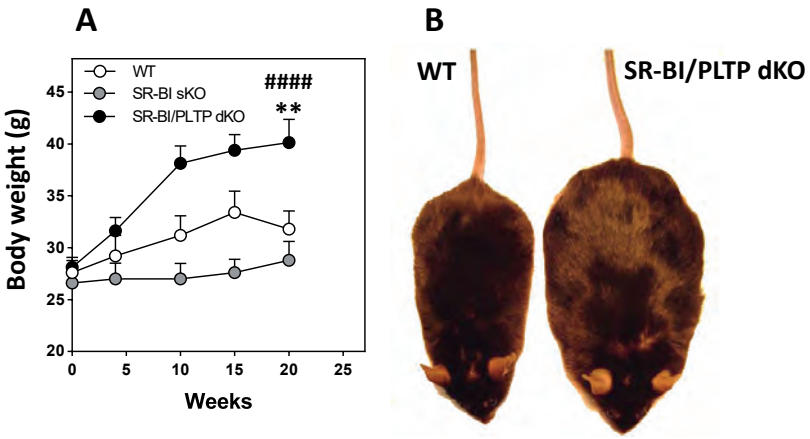

Figure 6: Over time WTD feeding altered the body weight of wild type (WT, open circle, n=5), SR-BI sKO (SR-BI sKO, grey circle, n=5) mice, and SR-BI/PLTP dKO (SR-BI/PLTP dKO, black circle,n=8) mice. At 20 weeks WTD feeding statistically significant difference was **P<0.01 vs WT; #### P<0.001 vs sKO (A). Visual differences between representative SR-BI sKO and SR-BI/PLTP dKO mice at the 20 weeks' time point (B).

and SR-BI sKO mice was 1.2 and 1.4-fold higher (SR-BI/PLTP dKO 40.1 ± 2.3 g; SR-BI sKO 28.8 ± 1.8 g; WT 31.8 ± 1.7 g; P<0.001 for SR-BI/PLTP dKO vs SR-BI sKO and WT). Consistent with Lino et al. ([55] 2015), throughout the experiment the SR-BI sKO mice remained significantly lighter (AUC SR-BI sKO 546.7 ± 10.6; WT 619.3 ± 13.5; P<0.001) (**Figure 6A**).
The rise in BW in the SR-BI/PLTP dKO mice was mainly the result of increased gonadal WAT (gWAT absolute weight; WT 1.30 ± 0.15 g; SR-BI sKO 1.22 ± 0.38 g; SR-BI/PLTP dKO 5.01 ± 0.46 g; P<0.001 vs WT, P<0.001 vs sKO respectively) (**Figure 7A)** and subcutaneous WAT (sWAT absolute weight; WT 0.38 ± 0.09 g; SR-BI sKO 0.33 ± 0.07 g; SR-BI/PLTP dKO 0.70 ± 0.047 g; P<0.01 vs WT, P<0.01 vs sKO) (**Figure 7B**). Well established is the link between obesity and increased plasma TG.

Here we measured a 2.0-fold (P<0.005) increase in circulating TG levels upon WTD feeding in the dKO group compared to the SR-BI sKO mice (**Table 1**). These augmented TG levels in serum of the SR-BI/PLTP dKO mice coincided with an increased AUC in the VLDL fraction (AUC SR-BI sKO 12.5; SR-BI/PLTP dKO 34.0, based on VLDL-C) (**Figure 1A WTD**). Analysis of the lipid content of the VLDL particles showed a dramatic increase in TG content at the expense of CE in VLDL of SR-BI/PLTP dKO mice as compared to VLDL from SR-BI sKO mice (TG 1.5-fold; CE 0.7-fold) (**Figure 7C**).

Table 1: Plasma cholesterol levels of total body depleted SR-BI KO mice with and without additional PLTP function. Data represents mean+SEM; significant difference *P<0.05, ***P<0.005, ****P<0.001 versus WT: #P<0.05, ##P<0.01, ###P<0.005, ####P<0.001 versus SR-BI KO.

	TC (mg/dL)	FC (mg/dL)	TG (mg/dL)	PL (mg/dL)	FC/CE ratio
CHOW					
WT	69±1.3	16±1.6	191±6.0	191.1±6.0	0.18±0.03
SR-BI sKO	175±5.4***	86±2.8***	251±6.1 *	251.4±6.1 ****	0.58±0.02****
SR-BI/PLP dKO	121±3.0***###	56±1.6***##	195±6.4 #	187.7±7.3 ####	0.52±0.03****
WTD					
WT	139±11.3	26±1.4	20.8±3.9	252.1±15,5	0.14±0.01
SR-BI sKO	338±22.4***	173±13.0 ***	48.6±3.3 ###	370.3±12.9 ****	0.62±0.04****
SR-BI/PLP dKO	195±6.8*###	97.1±3.1 ***###	99.7±8.4 ****	267.5±7.7###	0.57±0.03****

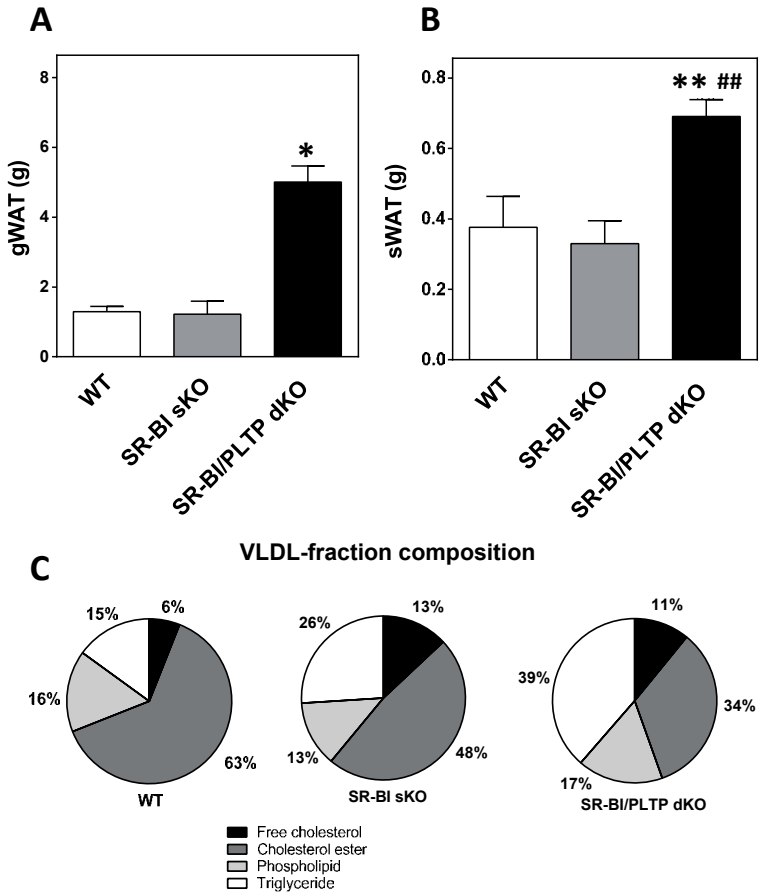

Figure 7: 20 weeks WTD fed SR-BI and PLTP depleted (SR-BI/PLPT dKO) mice displayed increased gonadal white adipose tissue (gWAT)(A), subcutaneous WAT (sWAT)(B). All data represents mean+SEM and statistically significant difference was *P<0.05, **P<0.01 vs WT; ## P<0.01 vs SRBI sKO. Very large density lipoprotein composition (fractions 2-6) upon WTD challenge in % (C).

Despite the elevated TG levels in the circulation and the increased gWAT and sWAT volume, no signs of nonalcoholic fatty liver disease were observed in the SR-BI/PLTP dKO mice. Moreover, the liver weights did not differ between the groups (absolute liver weight; SR-BI/PLTP dKO 1.8 ± 0.18 g, SR-BI sKO 1.4 ± 0.26 g; WT 1.7 ± 0.23 g; P<0.05 SR-BI/PLTP vs SR-BI sKO (**Figure 8A**). In addition, a clear SR-BI sKO hepatic lipid composition phenotype was observed, characterized by decreased levels of TC, FC, CE, PL and TG versus the WT group (**Figure 8B**).

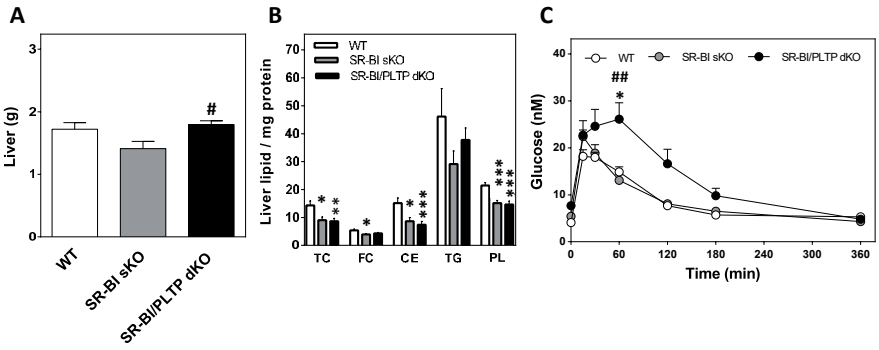

Figure 8: The effect of total body depletion of SR-BI (SR-BI sKO) and additional PLTP depletion (SR-BI/PLTP dKO) after 20 weeks WTD feeding on liver weight (A) liver lipid composition (B). The time course for a glucose tolerance test in response to a glucose bolus (C). Data represents mean+SEM (WTD n=5, SR-BI sKO n=5 and SR-BI/PLTP dKO n=8). Statistical difference of *P<0.05, **P<0.01, ***P<0.005 vs WT, ##P<0.01 versus SR-BI sKO.

Obesity is often associated with an disturbed glucose tolerance and an increased risk for type 2 diabetes mellitus [56]. In a glucose tolerance test, the SR-BI/PLTP dKO mice with an increased WAT volume displayed a worsened glucose handling with a 1.8-fold higher peak concentration at 60 min (t=60min SR-BI/PLTP dKO 26.1 ± 3.5 nM, SR-BI sKO 13.1 ± 1.2 nM, WT 14.9 ± 1.1 nM; SR-BI/PLTP dKO vs WT P<0.05, SR-BI/PLTP dKO vs SR-BI sKO P<0.01). At 360 minutes post glucose bolus, a normalization of blood glucose was recorded in all groups (t=360min SR-BI/PLTP dKO 4.8 ± 0.4 nM; SR-BI sKO 4.3 ± 0.3 nM; WT 5.3 ± 0.2 nM; P=NS) (**Figure 8C**). These data imply that the dKO mice display important signs of MetS [57] after 20 weeks WTD challenge, including elevated plasma TG levels, increased WAT volume and worsened glucose tolerance.

Next, we aimed to understand the role of PLTP in lipolysis and the link with the MetS-like phenotype observed in our SR-BI/PLTP dKO mice. Hereto a dedicated second experiment was performed on regular CHOW diet. In addition to WT, SR-BI sKO, and SR-BI/PLTP dKO mice also PLTP sKO mice were included, as to our knowledge until now no link between single PLTP deficiency and TG levels has been described. Consistent with the first study, TC values were lowered upon deletion of PLTP in SR-BI sKO mice (**Table 1 and 3**). Plasma TC levels of the PLTP sKO mice group were at WT level (**Table 3**). Under these CHOW-fed conditions TG levels (**Table 3**) and body weights (**Table 2**) were not significantly different amongst the different groups. Moreover, an oral glucose tolerance test showed no altered glucose sensitivity amongst the groups (AUC WT 69.5; SR-BI sKO 60.95; PLTP sKO 65.4; SR-BI/PLTP dKO 70.9) (**Figure 9A**).

Table 2: Organ and body weights of total body depleted SR-BI KO mice with and without additional PLTP function. Data represents mean+SEM; significant difference *P<0.05, **P<0.01, ***P<0.005 versus WT: ##P<0.01, ###P<0.005 versus SR-BI KO: $$$P<0.005 versus PLTP KO.

	BW	Liver	Spleen	Thymus	Adrenal	gWAT	iBAT	Heart
CHOW								
WT	25.8±0.88	1.25±0.044	0.10±0.008	0.03±0.005	0.02±0.001	0.82±0.014	0.06±0.004	0.14±0.006
SR-BI sKO	27.8±1.00	1.54±0.029	0.16±0.026*	0.04±0.006	0.02±0.003	0.68±0.092	0.07±0.004	0.17±0.011
PLTP sKO	28.8±0.09	1.35±0.083	0.11±0.013	0.06±0.0002**	0.07±0.001	1.35±0.300	0.06±0.005	0.15±0.015
SR-BI/PLTP dKO	31.0±1.98	1.59±0.085**	0.15.010*	0.05±0.006*	0.02±0.002	1.84±0.278**##	0.10±0.005***###$$$	0.15±0.010

Table 3: Plasma cholesterol levels of CHOW fed total body depleted SR-BI KO, PLTP KO and SR-BI/PLTP dKO mice. Data represents mean+SEM; significant difference *P<0.05, ****P<0.001 versus WT: ##P<0.01, ####P<0.001 versus SR-BI KO: $P<0.05, $$$P<0.005, $$$$P<0.001 versus PLTP KO.

	TC (mg/dL)	FC (mg/dL)	TG (mg/dL)	FC/CE ratio
CHOW				
WT	60.7±2.0	22.9±2.2	105.9±7.7	0.55±0.06
SR-BI sKO	162.9±5.1****	96.7±2.7****	88.5±9.5	1.49±0.03****
PLTP sKO	59.6±6.6####	28.3±2.8####	128.8±14.5	0.91±0.05* ##
SR-BI/PLTP dKO	114.1±7.6**** $$$	63.8±3.9**** #### $$$$	106.7±6.9	1.31±0.11**** $

Thus, the MetS-like phenotype in the SR-BI/PLTP dKO mice or underlying pathologies are not evident while feeding a regular CHOW diet with a low fat content. This allowed us to investigate if disruption of PLTP function in the SR-BI sKO mice was associated with any inherent disturbances in the metabolism of TG-rich lipoproteins independent of secondary effects.

Previous studies by Out et al. [58] showed that SR-BI facilitates the clearance of chylomicron remnants. In line with Out et al. a delayed TG response was observed in the SR-BI sKO after intragastric administration of an olive oil bolus after a 4 hour fasting period (t=3 h plasma ΔTG response; SR-BI sKO 0.29 ± 0.08 μg/μl; WT -0.07 ± 0.05 μg/μl; P<0.05), although the AUC was not affected (AUC SR-BI sKO 3.7 ± 0.2, WT 3.2 ± 0.2; P=NS). Interestingly, the PLTP sKO mice showed an even more dramatically increased plasma TG accumulation versus WT over time after olive oil administration (t=3 h plasma ΔTG response; PLTP sKO 0.45 ± 0.12 μg/μl; P<0.005 vs WT). Deletion of PLTP in the SR-BI sKO mice led to a further aggravation of the phenotype as evidenced by a 12-fold higher accumulation of TG in the circulation at the 3 hour time point (t=3 h plasma ΔTG response; SR-BI/PLTP dKO 0.85 ± 0.16 μg/μl; P<0.001 vs WT, P<0.05 vs PLTP sKO) (**Figure 9B**). In line with the augmented TG buildup over time in the PLTP sKO mice, a 1.4-fold increase was found in the AUC versus WT mice (AUC PLTP sKO 4.5 ± 0.5; P<0.05 vs WT). The SR-BI/PLTP dKO mice showed a further aggravated phenotype with a 1.7-fold increased AUC (AUC PLTP sKO 4.5 ± 0.5; P<0.001 versus WT, P<0.005 vs SR-BI sKO, P<0.05 vs SR-BI sKO) (**Figure 9C**)

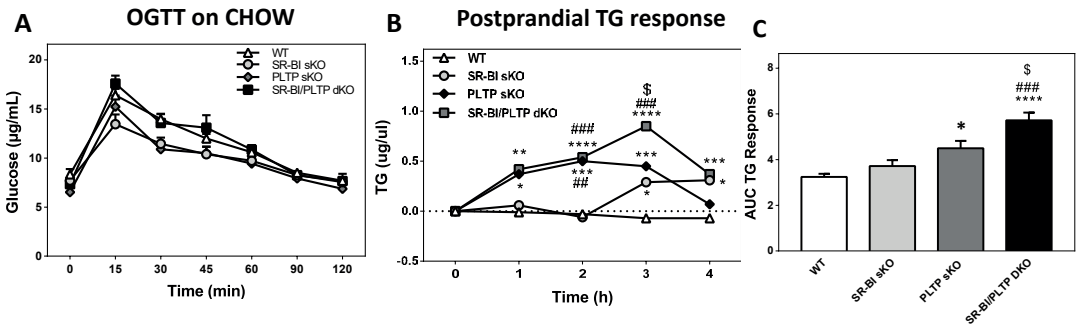

Figure 9: The time course of (A) glucose levels in response to a glucose bolus. TG levels upon a post prandial challenge with olive oil; over time (B), area under the curve (C). Data represents mean+SEM, **P<0.01, ***P<0.005, ****P<0.001 versus WT, #P<0.05, ##P<0.01 versus SR-BI sKO, $P<0.05, $$P<0.01 versus PLTP sKO.

Accumulation of TG in serum after an intragastric olive oil bolus is the nett effect of 1) absorption of TG in the intestine, 2) lipolysis of the TG-rich chylomicrons once in the circulation, and 3) removal of the particles and released free fatty acids from the circulation by tissues. Next, an in vivo clearance study was performed using triglyceride-rich VLDL-like particles, radiolabeled with glycerol [^{3}H]oleate ([^{3}H]TO) and [^{14}C]cholesteryl oleate ([^{14}C]CO), injected intravenously allowing investigation of the metabolism of these particles and tracing of their core lipids in time. [^{3}H]TO clearance from the plasma compartment was somewhat slower in PLTP KO and DKO mice as compared to both SR-BI KO and WT mice with average plasma half-lives of 5.4 and 4.0 minutes versus 2.5 and 2.3 minutes, respectively (**Figure 10A**). The associated [^{3}H]TO elimination rate constants (K) were 0.30 ± 0.10 for WT mice, 0.28 ± 0.07 for SR-BI KO mice, 0.13 ± 0.04 for PLTP KO mice, and 0.17 ± 0.10 for DKO mice (**Figure 10B**). This observation is in line with our previous findings that the plasma lipoprotein lipase (LPL) and hepatic lipase (HL) activity is similar in SR-BI KO and wild-type mice [60]. Given the general short plasma half-life of [^{3}H]TO, it is not surprising that upon sacrifice, i.e. at 15 minutes after particle injection, no difference was found amongst the different genotype groups in the uptake of [^{3}H]TO by the primary target organs heart and liver (**Figure 10C**). In accordance with the notion that in WT mice VLDL/chylomicron-remnants are rapidly cleared from the circulation, the plasma half-life of the [^{14}C]CO tracer (2.6 minutes; K: 0.26 ± 0.11) was almost similar to that of the [^{3}H]TO tracer (2.3 minutes: K: 0.30 ± 0.10; **Figures 10A & B**). In contrast, [^{14}C]CO plasma clearance was slower than that of [^{3}H]TO in SR-BI KO mice (average half-life: 3.6 minutes; K: 0.19 ± 0.0.09 for [^{14}C]CO versus 2.5 minutes; K: 0.28 ± 0.07 for [^{3}H]TO;

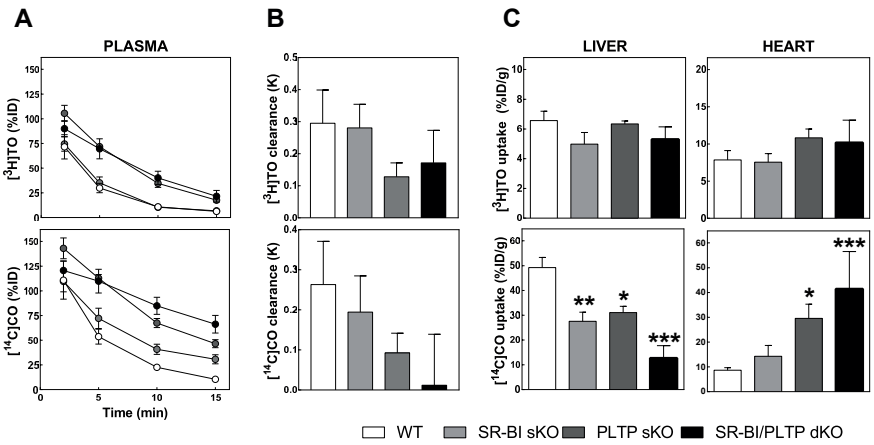

Figure 10: Plasma decay (A) and tissue uptake (C) of radiolabeled triglyceride-rich lipoprotein-associated fatty acids ([^{3}H]TO-derived activity) and cholesteryl esters ([^{14}C]CO) in chow diet–fed male mice. The calculated plasma clearance rates are shown in (B). *P<0.05, **P<0.01, ***P<0.001 vs WT.

Figures 10A & B). In further support of the suggested impact of SR-BI deficiency on the uptake of chylomicron- and VLDL-remnants by hepatocytes [59, 60], a significantly lower amount of [^{14}C]CO was recovered in SR-BI KO livers as compared to WT livers at 15 minutes after triglyceride-rich particle administration (-44 %; P<0.001; **Figure 10C**). The plasma clearance of [^{14}C]CO was also markedly delayed in PLTP KO mice (average plasma half-life: 7.5 minutes; K: 0.09 ± 0.05; **Figures 10A & B**) and this was paralleled by a reduced hepatic remnant particle uptake at 15 minutes after injection (-37 %; P<0.001). Strikingly, remnant particle clearance was even further delayed in DKO mice with an average [^{14}C]CO plasma half-life of 58 minutes (K: 0.01 ± 0.13; **Figures 10A & B**). As a result, livers of DKO mice had taken up only 26 % of the fractional dose of [^{14}C]CO that could be recovered in WT livers at 15 minutes after intravenous particle injection (P<0.001; **Figure 10C**). In contrast, a relatively high level of [^{14}C]CO tracer was detected in hearts of PLTP and DKO mice (**Figure 10C**).

Given that we have previously found that SR-BI deficiency does not alter hepatic expression levels of other receptors involved in lipoprotein remnant uptake, i.e. the LDL receptor and LDL receptor-related protein 1 (LRP1) [60], it can be suggested that in response to the PLTP deficiency a VLDL-remnant particle is generated that is highly dependent on SR-BI for its subsequent clearance by hepatocytes and therefore ultimately accumulates in alternative tissues in a SR-BI deficiency setting.

DISCUSSION

Key findings of this study are A) Deletion of PLTP reduced the SR-BI KO specific enlarged HDL particle size and B) SR-BI/PLTP dKO mice displayed a lower susceptibility to atherosclerosis despite the development of a MetS-like phenotype driven by a defect in TG lipolysis induced by the absence of PLTP. In our unique double knockout mouse model the occurrence of MetS is thus uncoupled from atherosclerosis susceptibility.

Deletion of PLTP in the SR-BI knockout background induced a massive reduction in the amount of large CE-rich HDL particles that accumulate as a result of hepatic SR-BI deficiency in these animals. This clearly indicates that the transfer of phospholipids, released during the lipolysis of TG in TG-rich lipoproteins, to HDL is essential for the enlargement of the HDL particles in SR-BI knockout mice. However, the formation of the HDL particles was not fully ablated. In line with the theory presented by Settasatian [40] we hypothesize that the remaining HDL fraction in SR-BI/PLTP dKO mice is the result of expansion of pre-β HDL particles to their maximum size of available surface PL, followed by fusion into larger CE-enriched particles through electron field differences [61]. This, in combination with the disturbed hepatic CE-uptake due to the SR-BI deficiency, resulted in the remaining levels of HDL in the circulation of SR-BI/PTLP dKO mice [62]. Further maturation of the HDL particles requires the intervention of PLTP and hence is no longer possible [63, 40].

In the general discussion about HDL, the balance tipped towards HDL functionality, not HDL-C quantity, especially for its` anti-atherogenic function [64]. HDL functionality in the reverse cholesterol transport route differs per subclass [65]. Here the in vitro data showed that plasma of the SR-BI/PLTP dKO mice with a smaller HDL particle size and quantity tends to be more effective in inducing macrophage cholesterol efflux over plasma of SR-BI sKO. Moreover, oxidative stress levels locally in the arterial wall were reduced, indicating that both the anti-oxidant and cholesterol efflux functionality of HDL was, at least partly, restored upon deletion of PLTP in the SR-BI KO mice. Atherosclerotic lesion development was however not fully prevented. While smal pre-β HDL particles effectively interact with ATP binding cassette reporter A1 (ABCA1) on macrophages to stimulate cholesterol efflux, ABCG1 and SR-BI facilitate efflux to large mature α-HDL particles [66]. The fact that atherosclerotic lesion development is not completed prevented might be a direct consequence of the absence of macrophage SR-BI. In line our group [67] and others [68,69] previously showed that deletion of SR-BI on bone marrow-derived cells induces atherosclerosis susceptibility of LDL receptor

knockout mice. On the other hand, one can argue that the impaired delivery of HDL's cholesterol cargo to the liver in absence of SR-BI and thus impairment of the last step of the RCT pathway might have been a causative factor in determining atherosclerosis susceptibility in the SR-BI/PLTP dKO mice. However, previous studies in ABCA1/SR-BI knockout mice showed that impairment of macrophage RCT is not sufficient to induce atherosclerotic lesion development [70]. The presence of pro-atherogenic lipoproteins, such as VLDL in the circulation is a prerequisite for atherosclerotic lesion development. Strikingly, SR-BI/PLTP dKO mice showed reduced atherosclerosis as compared to SR-BI sKO mice, despite increased levels of TG-rich VLDL and the development of a MetS-like phenotype (increased WAT, TG and altered fasting glucose levels) [71]. Generally, the presence of MetS is associated with an increased risk for CVD in both humans and mice [72,73]. Our study is one of the first to show an uncoupling between MetS phenotype and atherosclerosis susceptibility.

We hypothesize that the augmented levels of plasma TG triggered the expansion of WAT and subsequently led to the glucose intolerance. Wang et al. indicated an important role for SR-BI in the hepatic clearance of TG enriched ApoB containing lipoproteins (VLDL and chylomicrons)[70,74]. In line, deletion of SR-BI in mice results in elevated levels of these TG-rich lipoproteins [75]. Previous findings of Karavia et al. and our current study show that this is however not associated with weight gain and adiposity of SR-BI sKO mice on WTD [76]. Thus, the additional PLTP deletion in the SR-BI KO background is critical for induction of the MetS phenotype.

High expression levels of PLTP are found in adipose tissue in both men and mice [77,78]. In line, plasma PLTP activity is increased in obese patients [79]. PLTP in adipocytes has been implicated in the promotion of cellular cholesterol efflux [80]. PLTP deletion in adipocytes could thus have led to a disturbed adipose cholesterol balance and subsequently increased body weight and development of a MetS phenotype on WTD. Although, PLTP knockout mice have been extensively studied, until now no effects of PLTP deficiency on body weight gain have been described. It is thus likely that the phenotype is not a direct effect of PLTP deficiency in the adipose tissue, but rather an effect of the massive increase in serum TGs in the SR-BI/PLTP dKOs. Jiang X et al. previously showed that PLTP sKO mice on WTD display no change in TG levels in blood [81]. It is therefore possible that the phenotype becomes only visible on WTD when the clearance of TG-rich lipoproteins and their remnants is impaired, like in the SR-BI KO mice that lack a hepatic recognition site for TG-rich lipoproteins and their remnants [75,82]. Here, we showed that the absence of PLTP did not affect LPL-

mediated triglyceride lipolysis, but rather modified the ability of VLDL/chylomicron remnants to be cleared from the circulation by the liver through receptors other than SR-BI. As a result, livers of DKO mice only cleared 26 % of the fractional dose of [^{14}C]cholesteryl oleate after intravenous triglyceride-rich particle injection. Further mechanistic studies are required to unequivocally establish this two-way dependency of PL transfer and TG lipolysis.

REFERENCES

1. Miller, G . J. & Miller, N. E. Plasma-high-density-lipoprotein concentration and development of ischæmic heart-disease. *Lancet* 305, 16-19 (1975).
2. Geff, W. B., Sull, M., Bart, W. & Malo, G. Protein-lipid Relationships in Human Plasma. II--. *Am. J. Med.* 4, (1951).
3. Gordon, D. J. & Rifkind, B. M. High-density lipoprotein--the clinical implications of recent studies. *N. Engl. J. Med.* 321, 1311-6 (1989).
4. Gordon, D. J. et al. High-density lipoprotein cholesterol and cardiovascular disease. Four prospective American studies. *Circulation* 79, 8-15 (1989).
5. Gordon, T., Castelli, W. P., Hjortland, M. C., Kannel, W. B. & Dawber, T. R. High density lipoprotein as a protective factor against coronary heart disease: The Framingham study. *Am. J. Med.* 62, 707-714 (1977).
6. Miller, N. E., Thelle, D. S., Førde, O. H. & Mjøs, O. D. The tromsøheart-study: high-density lipoprotein and coronary heart-disease: a prospective case-control study. *Lancet* 309, 965-968 (1977).
7. Jin, W., Millar, J. S., Broedl, U., Glick, J. M. & Rader, D. J. Inhibition of endothelial lipase causes increased HDL cholesterol levels in vivo. *J. Clin. Invest.* 111, 357-62 (2003).
8. Ishida, T. et al. Endothelial lipase modulates susceptibility to atherosclerosis in apolipoprotein-E-deficient mice. *J. Biol. Chem.* 279, 45085-92 (2004).
9. Bérard, A. M. et al. High plasma HDL concentrations associated with enhanced atherosclerosis in transgenic mice overexpressing lecithinchoesteryl acyltransferase. *Nat. Med.* 3, 744-749 (1997).
10. Braun, A. et al. Loss of SR-BI expression leads to the early onset of occlusive atherosclerotic coronary artery disease, spontaneous myocardial infarctions, severe cardiac dysfunction, and premature death in apolipoprotein E-deficient mice. *Circ. Res.* 90, 270-6 (2002).
11. Ameli, S. et al. Recombinant apolipoprotein A-I Milano reduces intimal thickening after balloon injury in hypercholesterolemic rabbits. *Circulation* 90, 1935-41 (1994).
12. Soma, M. R. et al. Recombinant apolipoprotein A-IMilano dimer inhibits carotid intimal thickening induced by perivascular manipulation in rabbits. *Circ. Res.* 76, 405-11 (1995).
13. Shah, P. K. et al. High-Dose Recombinant Apolipoprotein A-IMilano Mobilizes Tissue Cholesterol and Rapidly Reduces Plaque Lipid and Macrophage Content in Apolipoprotein E-Deficient Mice : Potential Implications for Acute Plaque Stabilization. *Circulation* 103, 3047-3050 (2001).
14. Shah, P. K. et al. Effects of recombinant apolipoprotein A-I(Milano) on aortic atherosclerosis in apolipoprotein E-deficient mice. *Circulation* 97, 780-5 (1998).
15. Chiesa, G. et al. Recombinant apolipoprotein A-I(Milano) infusion into rabbit carotid artery rapidly removes lipid from fatty streaks. *Circ. Res.* 90, 974-80 (2002).
16. Chyu, K.-Y. & Shah, P. K. HDL/ApoA-1 infusion and ApoA-1 gene therapy in atherosclerosis. *Front. Pharmacol.* 6, 187 (2015).
17. Barter, P. J. et al. Effects of Torcetrapib in Patients at High Risk for Coronary Events. *N. Engl. J. Med.* 357, 2109-2122 (2007).
18. Fayad, Z. A. et al. Safety and efficacy of dalcetrapib on atherosclerotic disease using novel non-invasive multimodality imaging (dal-PLAQUE): a randomised clinical trial. *Lancet* 378, 1547-1559 (2011).
19. Teo, K. K. et al. Extended-Release Niacin Therapy and Risk of Ischemic Stroke in Patients With Cardiovascular Disease: The Atherothrombosis Intervention in Metabolic Syndrome With Low HDL/High Triglycerides: Impact on Global Health Outcome (AIM-HIGH) Trial. *Stroke* 44, 2688-2693 (2013).
20. Haynes, R. et al. HPS2-THRIVE randomized placebo-controlled trial in 25 673 high-risk patients of ER niacin/laropiprant: trial design, pre-specified muscle and liver outcomes, and reasons for stopping study treatment. *Eur. Heart J.* 34, 1279-1291 (2013).

21. HPS3/TIMI55-REVEAL Collaborative Group et al. Effects of Anacetrapib in Patients with Atherosclerotic Vascular Disease. *N. Engl. J. Med.* 377, 1217-1227 (2017).
22. Nakagawa-Toyama, Y. et al. Human scavenger receptor class B type I is expressed with cell-specific fashion in both initial and terminal site of reverse cholesterol transport. *Atherosclerosis* 183, 75-83 (2005).
23. Wang, N., Weng, W., Breslow, J. L. & Tall, A. R. Scavenger receptor BI (SR-BI) is up-regulated in adrenal gland in apolipoprotein A-I and hepatic lipase knock-out mice as a response to depletion of cholesterol stores. In vivo evidence that SR-BI is a functional high density lipoprotein receptor under feedback control. *J. Biol. Chem.* 271, 21001-4 (1996).
24. Landschulz, K. T., Pathak, R. K., Rigotti, A., Krieger, M. & Hobbs, H. H. Regulation of scavenger receptor, class B, type I, a high density lipoprotein receptor, in liver and steroidogenic tissues of the rat. *J. Clin. Invest.* 98, 984-95 (1996).
25. Fluiter, K., van der Westhuijzen, D. R. & van Berkel, T. J. In vivo regulation of scavenger receptor BI and the selective uptake of high density lipoprotein cholesteryl esters in rat liver parenchymal and Kupffer cells. *J. Biol. Chem.* 273, 8434-8 (1998).
26. Adorni, M. P. et al. The roles of different pathways in the release of cholesterol from macrophages. *J. Lipid Res.* 48, 2453-62 (2007).
27. Vergeer, M. et al. Genetic Variant of the Scavenger Receptor BI in Humans. *N Engl J Med* 364, 136-45 (2011).
28. Zanoni, P. Rare variant in scavenger receptor BI raises HDL cholesterol and increases risk of coronary heart disease. *Science* (80-.). 351, 1166-1171 (2016).
29. Chadwick, A. C. & Sahoo, D. Functional Characterization of Newly-Discovered Mutations in Human SR-BI. *PLoS One* 7(9):e45660. (2012).
30. Brunham, L. R. et al. Novel mutations in scavenger receptor BI associated with high HDL cholesterol in humans. *Clin. Genet.* 79, 575-581 (2011).
31. West, M. et al. Scavenger Receptor Class B Type I Protein as an Independent Predictor of High-Density Lipoprotein Cholesterol Levels in Subjects with Hyperalphalipoproteinemia. *J. Clin. Endocrinol. Metab.* 94, 1451-1457 (2009).
32. Hsu, L. A. et al. Association between a novel 11-base pair deletion mutation in the promoter region of the scavenger receptor class B type I gene and plasma HDL cholesterol levels in Taiwanese Chinese. *Arterioscler. Thromb. Vasc. Biol.* 23, 1869-1874 (2003).
33. Rigotti, A. et al. A targeted mutation in the murine gene encoding the high density lipoprotein (HDL) receptor scavenger receptor class B type I reveals its key role in HDL metabolism. *Proc. Natl. Acad. Sci. U. S. A.* 94, 12610-5 (1997).
34. Kozarsky, K. F. et al. Overexpression of the HDL receptor SR-BI alters plasma HDL and bile cholesterol levels. *Nature* 387, 414-417 (1997).
35. Van Eck, M. et al. Differential effects of scavenger receptor BI deficiency on lipid metabolism in cells of the arterial wall and in the liver. *J. Biol. Chem.* 278, 23699-23705 (2003).
36. Tu, A. Y., Nishida, H. I. & Nishida, T. High density lipoprotein conversion mediated by human plasma phospholipid transfer protein. *J. Biol. Chem.* 268, 23098-105 (1993).
37. Albers, J. J. et al. Functional expression of human and mouse plasma phospholipid transfer protein: effect of recombinant and plasma PLTP on HDL subspecies. *Biochim. Biophys. Acta* 1258, 27-34 (1995).
38. van Tol, A. Phospholipid transfer protein. *Curr. Opin. Lipidol.* 13, 135-9 (2002).
39. Jauhiainen, M. et al. Human plasma phospholipid transfer protein causes high density lipoprotein conversion. *J. Biol. Chem.* 268, 4032-6 (1993).
40. Settasatian, N. et al. The mechanism of the remodeling of high density lipoproteins by phospholipid transfer protein. *J. Biol. Chem.* 276, 26898-905 (2001).
41. Hoekstra, M., Kruijt, J. K., Van Eck, M. & Van Berkel, T. J. C. Specific gene expression of ATP-binding cassette transporters and nuclear hormone receptors in rat liver parenchymal, endothelial, and Kupffer cells. *J. Biol. Chem.* 278, 25448-53 (2003).

42. van der Sluis, R. J., Nahon, J. E., Reuwer, A. Q., Van Eck, M. & Hoekstra, M. Haloperidol inhibits the development of atherosclerotic lesions in LDL receptor knockout mice. *Br. J. Pharmacol.* 172, 2397-405 (2015).
43. Praticò, D., Tangirala, R. K., Rader, D. J., Rokach, J. & FitzGerald, G. A. Vitamin E suppresses isoprostane generation in vivo and reduces atherosclerosis in ApoE-deficient mice. *Nat. Med.* 4, 1189-92 (1998).
44. Stackman, R. W. et al. Prevention of age-related spatial memory deficits in a transgenic mouse model of Alzheimer's disease by chronic Ginkgo biloba treatment. *Exp. Neurol.* 184, 510-20 (2003).
45. Redgrave, T. G., Roberts, D. C. K. & West, C. E. Separation of plasma lipoproteins by density-gradient ultracentrifugation. *Anal. Biochem.* 65, 42-49 (1975).
46. Rensen, P. C. et al. Selective liver targeting of antivirals by recombinant chylomicrons--a new therapeutic approach to hepatitis B. *Nat. Med.* 1, 221-5 (1995).
47. Jong, M. C. et al. Apolipoprotein C-III deficiency accelerates triglyceride hydrolysis by lipoprotein lipase in wild-type and apoE knockout mice. *J. Lipid Res.* 42, 1578-85 (2001).
48. Rigotti, A. et al. A targeted mutation in the murine gene encoding the high density lipoprotein (HDL) receptor scavenger receptor class B type I reveals its key role in HDL metabolism. *Proc. Natl. Acad. Sci. U. S. A.* 94, 12610-5 (1997).
49. Meurs, I. et al. HDL cholesterol levels are an important factor for determining the lifespan of erythrocytes. *Exp. Hematol.* 33, 1309-1319 (2005).
50. Huuskonen, J. et al. Phospholipid Transfer Is a Prerequisite for PLTP-Mediated HDL Conversion. *Biochemistry* 51, 16092-8 (2000).
51. Brundert, M. et al. Selective uptake of HDL cholesteryl esters and cholesterol efflux from mouse peritoneal macrophages independent of SR-BI. *J. Lipid Res.* 47, 2408-21 (2006).
52. Korporaal, S. J. A. et al. Deletion of the high-density lipoprotein receptor scavenger receptor BI in mice modulates thrombosis susceptibility and indirectly affects platelet function by elevation of plasma free cholesterol. *Arterioscler. Thromb. Vasc. Biol.* 31, 34-42 (2011).
53. Van Eck, M. et al. Increased oxidative stress in scavenger receptor BI knockout mice with dysfunctional HDL. *Arterioscler. Thromb. Vasc. Biol.* 27, 2413-9 (2007).
54. Praticò, D. Prostanoid and isoprostanoid pathways in atherogenesis. *Atherosclerosis* 201, 8-16 (2008).
55. Lino, M. et al. Intestinal scavenger receptor class B type I as a novel regulator of chylomicron production in healthy and diet-induced obese states. *Am. J. Physiol. Gastrointest. Liver Physiol.* 309, G350-9 (2015).
56. Kahn, S. E., Hull, R. L. & Utzschneider, K. M. Mechanisms linking obesity to insulin resistance and type 2 diabetes. *Nature* 444, 840-846 (2006).
57. Vollenweider, P., von Eckardstein, A. & Widmann, C. in *Handb Exp Pharmacol.* 405-421 (2015).
58. Out, R. et al. Scavenger receptor class B type I is solely responsible for the selective uptake of cholesteryl esters from HDL by the liver and the adrenals in mice. *J. Lipid Res.* 45, 2088-95 (2004).
59. Van Eck, M. et al. Scavenger receptor BI facilitates the metabolism of VLDL lipoproteins in vivo. *J Lipid Res.*49:136–146. (2008).
60. Out, R. et al. Scavenger receptor BI plays a role in facilitating chylomicron metabolism. *J Biol Chem.* 279:18401–18406. (2004)
61. Webb, N. R. et al. Remodeling of HDL remnants generated by scavenger receptor class B type I. *J. Lipid Res.* 45, 1666-73 (2004).
62. Lee, J.-Y. et al. Prebeta high density lipoprotein has two metabolic fates in human apolipoprotein A-I transgenic mice. *J. Lipid Res.* 45, 716-28 (2004).
63. Lusa, S., Jauhiainen, M., Metso, J., Somerharju, P. & Ehnholm, C. The mechanism of human plasma phospholipid transfer protein-induced enlargement of high-density lipoprotein particles: evidence for particle fusion. *Biochem. J.* 313, 275-82 (1996).

64. Rohatgi, A. et al. HDL Cholesterol Efflux Capacity and Incident Cardiovascular Events. *N. Engl. J. Med.* 371, 2383-2393 (2014).
65. Cavigiolio, G. et al. The Interplay between Size, Morphology, Stability, and Functionality of High-Density Lipoprotein Subclasses. *Biochemistry* 47, 4770-4779 (2008).
66. Rothblat, G. H. & Phillips, M. C. High-density lipoprotein heterogeneity and function in reverse cholesterol transport. *Curr. Opin. Lipidol.* 21, 229-38 (2010).
67. Zhao, Y. et al. Enhanced Foam Cell Formation, Atherosclerotic Lesion Development, and Inflammation by Combined Deletion of ABCA1 and SR-BI in Bone Marrow-Derived Cells in LDL Receptor Knockout Mice on Western-Type Diet. *Circ. Res.* 107, e20-e31 (2010).
68. Stangl, H., Cao, G., Wyne, K. L. & Hobbs, H. H. Scavenger receptor, class B, type I-dependent stimulation of cholesterol esterification by high density lipoproteins, low density lipoproteins, and nonlipoprotein cholesterol. *J. Biol. Chem.* 273, 31002-8 (1998).
69. Huszar, D. et al. Increased LDL cholesterol and atherosclerosis in LDL receptor-deficient mice with attenuated expression of scavenger receptor B1. *Arterioscler. Thromb. Vasc. Biol.* 20, 1068-73 (2000).
70. Zhao, Y. et al. Hypocholesterolemia, foam cell accumulation, but no atherosclerosis in mice lacking ABC-transporter A1 and scavenger receptor BI. *Atherosclerosis* 218, 314-22 (2011).
71. Kennedy, A. J., Ellacott, K. L. J., King, V. L. & Hasty, A. H. Mouse models of the metabolic syndrome. *Dis. Model. Mech.* 3, 156-66 (2010).
72. McGarry, J. D. What if Minkowski had been ageusic? An alternative angle on diabetes. *Science* 258, 766-70 (1992).
73. Isomaa, B. et al. Cardiovascular morbidity and mortality associated with the metabolic syndrome. *Diabetes Care* 24, 683-9 (2001).
74. Wang, N., Arai, T., Ji, Y., Rinninger, F. & Tall, A. R. Liver-specific overexpression of scavenger receptor BI decreases levels of very low density lipoprotein ApoB, low density lipoprotein ApoB, and high density lipoprotein in transgenic mice. *J. Biol. Chem.* 273, 32920-6 (1998).
75. Van Eck, M. et al. Scavenger receptor BI facilitates the metabolism of VLDL lipoproteins in vivo. *J. Lipid Res.* 49, 136-46 (2008).
76. Karavia, E. A. et al. Scavenger Receptor Class B Type I Regulates Plasma Apolipoprotein E Levels and Dietary Lipid Deposition to the Liver. *Biochemistry* 54, 5605-5616 (2015).
77. Jiang, X. C. & Bruce, C. Regulation of murine plasma phospholipid transfer protein activity and mRNA levels by lipopolysaccharide and high cholesterol diet. *J. Biol. Chem.* 270, 17133-8 (1995).
78. Dusserre, E., Moulin, P. & Vidal, H. Differences in mRNA expression of the proteins secreted by the adipocytes in human subcutaneous and visceral adipose tissues. *Biochim. Biophys. Acta - Mol. Basis Dis.* 1500, 88-96 (2000).
79. Dullaart, R. P. F., Vergeer, M., de Vries, R., Kappelle, P. J. W. H. & Dallinga-Thie, G. M. Type 2 diabetes mellitus interacts with obesity and common variations in PLTP to affect plasma phospholipid transfer protein activity. *J. Intern. Med.* 271, 490-498 (2012).
80. Jiang, H. et al. Adipocyte phospholipid transfer protein and lipoprotein metabolism. *Arterioscler. Thromb. Vasc. Biol.* 35, 316-22 (2015).
81. Jiang, X. C. et al. Apolipoprotein B secretion and atherosclerosis are decreased in mice with phospholipid-transfer protein deficiency. *Nat. Med.* 7, 847-52 (2001).
82. Out, R. et al. Scavenger receptor class B type I is solely responsible for the selective uptake of cholesteryl esters from HDL by the liver and the adrenals in mice. *J. Lipid Res.* 45, 2088-95 (2004).

Division of BioTherapeutics, Leiden Academic Centre for Drug Research,
Leiden, The Netherlands

Atherosclerosis. 278:240-249 (2018)